Modified Chaishao Liujunzi Decoction Improving Metabolic Dysfunction-associated Steatotic Liver Disease through Regulating Nrf2/HO-1 Pathway

Minling JIANG[1], Hui WEN[1], Wu HE[1], Jian YANG[1], Kefeng ZHANG[2]

1. The First Affiliated Hospital of Guilin Medical University, Guilin 541001, China; 2. Key Laboratory of Pharmacology for Prevention and Treatment of High Incidence Diseases in Guangxi Higher Education Institutions, Guilin Medical University, Guilin 541199, China

Abstract [**Objectives**] To investigate the ameliorative effects of Modified Chaishao Liujunzi Decoction (MCLD) on metabolic dysfunction-associated steatotic liver disease (MASLD) and its regulatory mechanism on the Nrf2/HO-1 pathway. [**Methods**] A MASLD model in C57BL/6J mice was induced by a high-fat diet (HFD) for 12 weeks. After successful modeling, the mice were randomly divided into a model group and an MCLD group (10 g/kg), with intragastric administration for 4 weeks. Serum levels of ALT, AST, TG, and TC, as well as hepatic contents of MDA, SOD, and GSH, were measured. Hepatic pathological changes were observed by HE and Oil Red O staining. The mRNA and protein expressions of hepatic Nrf2, HO-1, and NQO1 were detected by qRT-PCR and Western blot. [**Results**] After MCLD intervention, hepatic steatosis and lipid accumulation were significantly alleviated. Serum ALT, AST, TG, TC and hepatic MDA content were markedly reduced ($P<0.05$), while SOD activity and GSH content were significantly increased ($P<0.05$). MCLD significantly upregulated the mRNA expressions of Nfe2l2, Hmox1, and Nqo1, as well as the protein expressions of Nrf2, HO-1, and NQO1 ($P<0.05$). [**Conclusions**] MCLD can improve HFD-induced MASLD by activating the hepatic Nrf2/HO-1/NQO1 antioxidant signaling pathway, enhancing antioxidant capacity, and reducing lipid peroxidation damage.

Key words Modified Chaishao Liujunzi Decoction (MCLD), Metabolic dysfunction-associated steatotic liver disease (MASLD), Nrf2/HO-1 signal pathway, Oxidative stress

1 Introduction

The primary pathological feature of metabolic dysfunction-associated steatotic liver disease (MASLD) is abnormal lipid deposition in hepatocytes, making it the chronic liver disorder with the highest number of affected patients globally[1-2]. In the progression of MASLD, oxidative stress is recognized as a key pathogenic hub linking lipid metabolic disturbances to hepatocellular damage[3]. In the MASLD state, large amounts of fatty acids accumulated within hepatocytes undergo β-oxidation to generate excessive reactive oxygen species (ROS), and the concomitant dysfunction of the mitochondrial respiratory chain further promotes ROS overproduction[4]. Once ROS levels overwhelm the clearance capacity of the endogenous antioxidant system, cellular membrane integrity is compromised and hepatocyte function becomes impaired[5]. Hence, strengthening antioxidative defenses and counteracting oxidative stress constitute a major direction for the treatment of MASLD.

Nuclear factor erythroid 2-related factor 2 (Nrf2) is a core transcription factor that regulates endogenous antioxidant responses and plays a critical role in maintaining cellular redox homeostasis[6]. Under resting conditions, Nrf2 is retained in the cytoplasm in an inactive form. Upon oxidative stimulation, Nrf2 translocates into the nucleus, binds to the antioxidant response element (ARE), and initiates the transcription of multiple downstream antioxidant enzymes and phase II detoxifying enzyme genes[7]. Among these, heme oxygenase-1 (HO-1) is one of the most representative target genes downstream of Nrf2; the biliverdin/bilirubin generated from heme degradation catalyzed by HO-1 possesses direct free-radical scavenging activity[8]. Quinone oxidoreductase 1 [NAD(P)H: quinone oxidoreductase 1, NQO1] is another important phase II detoxifying enzyme that reduces toxic quinones to less toxic hydroquinones, thereby diminishing ROS production mediated by redox cycling[9]. Studies have shown that activation of the Nrf2/HO-1/NQO1 signaling axis can significantly alleviate hepatic lipid peroxidation injury and improve MASLD[10-11]. Therefore, the Nrf2/HO-1/NQO1 pathway has become a central target pathway in pharmacological intervention research for MASLD.

Modified Chaishao Liujunzi Decoction (MCLD) is a formula derived from Chaishao Liujunzi Decoction recorded in Volume 51 of *Golden Mirror of Medicine* (Yi Zong Jin Jian), with modifications based on specific disease manifestations and patient constitution. It is composed of Codonopsis Radix (Dangshen), Atractylodis Macrocephalae Rhizoma (Baizhu), Poria (Fuling), Bupleuri Radix (Chaihu), Paeoniae Radix Alba (Baishao), Citri Reticulatae Pericarpium (Chenpi), Pinelliae Rhizoma (Banxia), Curcumae Rhizoma (Ezhu), Salviae Miltiorrhizae Radix et Rhizoma (Danshen), Taraxaci Herba (Pugongying), Scutellariae Barbatae Herba (Banzhilian), Glycyrrhizae Radix et Rhizoma (Gancao), and Hedyotidis Diffusae Herba (Baihuasheshecao). The decoction has the effects of soothing the liver and strengthening the spleen. Clinical studies have confirmed that MCLD can effectively improve the clinical symptoms and liver function in patients with metabolic dysfunction-associated steatotic liver disease of the liver-stagnation and spleen-deficiency pattern. Furthermore, studies have shown

Received: June 4, 2026 Accepted: August 13, 2026
Supported by the Self-funded Research Project of Guangxi Administration of Traditional Chinese Medicine (GXZYZ20210091).

that the main components of MCLD can significantly alleviate hepatic steatosis and regulate lipid metabolism in mice[12]. However, whether MCLD can ameliorate MASLD through activation of the Nrf2/HO-1/NQO1 signaling pathway remains unclear.

Given the foregoing background, we established a high-fat diet (HFD)-induced mouse model of MASLD to systematically assess the hepatoprotective efficacy of MCLD. Besides, we explored the underlying molecular mechanism by which MCLD ameliorates MASLD via the Nrf2/HO-1/NQO1 signaling axis, with the aim of offering novel insights and experimental evidence for MASLD therapy.

2 Materials and methods

2.1 Experimental drugs MCLD consists of thirteen herbal medicines with the following quantities: Codonopsis Radix (Dangshen) 30 g, Atractylodis Macrocephalae Rhizoma (Baizhu) 15 g, Poria (Fuling) 15 g, Bupleuri Radix (Chaihu) 15 g, Paeoniae Radix Alba (Baishao) 15 g, Citri Reticulatae Pericarpium (Chenpi) 10 g, Pinelliae Rhizoma (Banxia) 9 g, Curcumae Rhizoma (Ezhu) 12 g, Salviae Miltiorrhizae Radix et Rhizoma (Danshen) 10 g, Taraxaci Herba (Pugongying) 15 g, Scutellariae Barbatae Herba (Banzhilian) 15 g, Glycyrrhizae Radix et Rhizoma (Gancao) 6 g, and Hedyotidis Diffusae Herba (Baihuasheshecao) 15 g. All crude drugs were sourced from the Guilin Chinese herbal medicine market and authenticated by Professor Zhang Kefeng of the School of Pharmacy, Guilin Medical University, meeting the specifications of the *Chinese Pharmacopoeia* (2020 Edition). The herbs were prepared into an aqueous decoction using an automatic decoction machine, and the pH was adjusted to 7.35. The decoction was filtered through 32-ply gauze, then centrifuged at 5 000 g for 20 min, with the centrifugation procedure repeated twice. The resulting supernatant was collected and passed through a 0.22-μm sterile disposable filter for sterilization. The sterile supernatant was then diluted to the required concentration, lyophilized into powder (yield: 20.78%), and preserved at −20 ℃.

2.2 Animal study Eight-week-old healthy C57BL/6J mice were housed in a specific pathogen-free (SPF) animal facility under controlled conditions of 22 − 26 ℃ and 40% − 60% relative humidity, with free access to food and water. After 1 week of adaptive feeding, the mice were randomly divided into a control group (Control, $n = 9$) and a HFD induction group ($n = 15$). Mice in the Control group were fed a standard diet daily, while those in the HFD group were fed a 60% HFD (XTHF60, Jiangsu Synergy Pharmaceutical Bioengineering Co., Ltd.) daily. After confirmation of successful model establishment, the HFD group was further randomly subdivided into an HFD group and an MCLD (10 g/kg) group[12]. Except for the Control group, the mice in the other two groups were maintained on the HFD. Meanwhile, the Control and HFD groups received an equal volume of distilled water by intragastric gavage daily, whereas the MCLD group received MCLD at the designated dose by gavage daily for 4 consecutive weeks. After the final administration, all mice were fasted for 16 h with free access to water, and then euthanized under anesthesia. Blood samples and liver tissues were collected for subsequent analyses of serum biochemical parameters, histopathology, and related assessments.

2.3 Histopathological examination Immediately following euthanasia, the mice were dissected to expose the liver; the gross morphology was examined and documented by photography. Liver specimens were fixed in 4% paraformaldehyde (or tissue fixative) for 48 h, processed through graded dehydration, clearing, paraffin embedding, and sectioning, and subsequently stained with hematoxylin and eosin (H&E) for histopathological evaluation. In addition, fresh liver samples were cryosectioned and subjected to Oil Red O (ORO) staining to assess the degree of hepatic lipid deposition.

2.4 Biochemical indicator assays Blood specimens were kept at 4 ℃ for 30 min and then centrifuged at 3 000 rpm for 15 min; the resulting sera were separated and preserved at −80 ℃. Serum concentrations of alanine aminotransferase (ALT, C009-2-1), aspartate aminotransferase (AST, C010-2-1), triglyceride (TG, A110-1-1), and total cholesterol (TC, A111-1-1) were assayed using commercial kits (Nanjing Jiancheng Bioengineering Institute) following the manufacturer's protocols. For hepatic tissue, samples were homogenized in ice-cold normal saline at a 1 ∶ 9 (*W/V*) ratio on ice, and the homogenates were centrifuged for 10 min to collect the supernatants. The levels of malondialdehyde (MDA, A003-1-2), superoxide dismutase (SOD, A001-3-2), and glutathione (GSH, A006-2-1) were measured in parallel from the same supernatants.

2.5 qRT-PCR Liver tissues collected from each group were added with 1 mL of Trizol and thoroughly lysed. After standing at room temperature for 5 min, chloroform and isopropanol were sequentially added to precipitate RNA according to the manufacturer's instructions, followed by washing with 75% ethanol and dissolution in DEPC-treated water. The obtained RNA samples were stored at −80 ℃ for later use. The concentration and purity of RNA were determined using the NanoDrop system. Subsequently, genomic DNA (gDNA) removal and reverse transcription were performed using the ToloScript ALL Reverse Transcription Kit according to the protocol. Quantitative polymerase chain reaction (qPCR) was carried out on the QuantStudio 3 qPCR system using the SYBR Green real-time PCR kit. The expression levels of target genes were normalized to the internal reference gene Actin, and the relative expression was calculated using the $2^{-\Delta\Delta Ct}$ method. The primer sequences used in the experiments are listed in Table 1.

Table 1 Primer sequence

Gene	Forward primer sequence(5′→3′)	Reverse primer sequence(5′→3′)
Nfe2l2	TCTTGGAGTAAGTCGAGAAGTGT	GTTGAAACTGAGCGAAAAAGGC
Hmox1	AAGCCGAGAATGCTGAGTTCA	GCCGTGTAGATATGGTACAAGGA
Nqo1	AGGATGGGAGGTACTCGAATC	AGGCGTCCTTCCTTATATGCTA
Actin	GGCTGTATTCCCCTCCATCG	CCAGTTGGTAACAATGCCATGT

2.6 Western blot analysis Liver tissues were lysed on ice with RIPA lysis buffer containing 1% PMSF for 30 min, then centrifuged at 12 000 r/min and 4 ℃ for 15 min. The middle-layer supernatant was collected, and the protein concentration was determined using the BCA method. Equal amounts of protein samples were subjected to SDS-PAGE for electrophoretic separation and then transferred onto NC membranes by the wet transfer method. The membranes were blocked with 5% non-fat milk at room temperature for 1 h, followed by incubation with specific primary antibodies overnight at 4 ℃. On the next day, after washing three times with TBST, the membranes were incubated with HRP-conjugated secondary antibodies at room temperature for 1 h. After thorough washing, the protein bands were visualized using ECL reagents and images were captured using a chemiluminescence imaging system (Table 2). B-ACTIN was used as the internal reference, and the relative expression levels of target proteins were calculated using ImageJ software.

Table 2 Antibodies

Name	Supplier	Location	Host	Cat no.	Dilution ratio
Nrf2	Proteintech	Wuhan, China	Rabbit	16396-1-AP	1∶5 000
HO-1	Proteintech	Wuhan, China	Rabbit	10701-1-AP	1∶6 000
NQO1	Proteintech	Wuhan, China	Rabbit	11451-1-AP	1∶8 000
β-ACTIN	Huabio	Huangzhou, China	Mouse	HA601585H	1∶5 000
IgG-HRP	Abmart	Shanghai, China	Goat	M21003S	1∶8 000

2.7 Statistical analysis All data were statistically analyzed using SPSS software. Results are expressed as mean ± standard deviation (Mean ± SD). For comparisons between two groups, an unpaired two-tailed Student's *t*-test was applied when the data met normal distribution and homogeneity of variances; otherwise, the Mann-Whitney U test was used. For comparisons among multiple groups, one-way analysis of variance (One-way ANOVA) followed by Dunnett's multiple comparison correction was performed when normality and homogeneity of variances were satisfied; otherwise, the non-parametric Kruskal-Wallis test was employed. A P-value < 0.05 was considered statistically significant.

3 Results and analysis

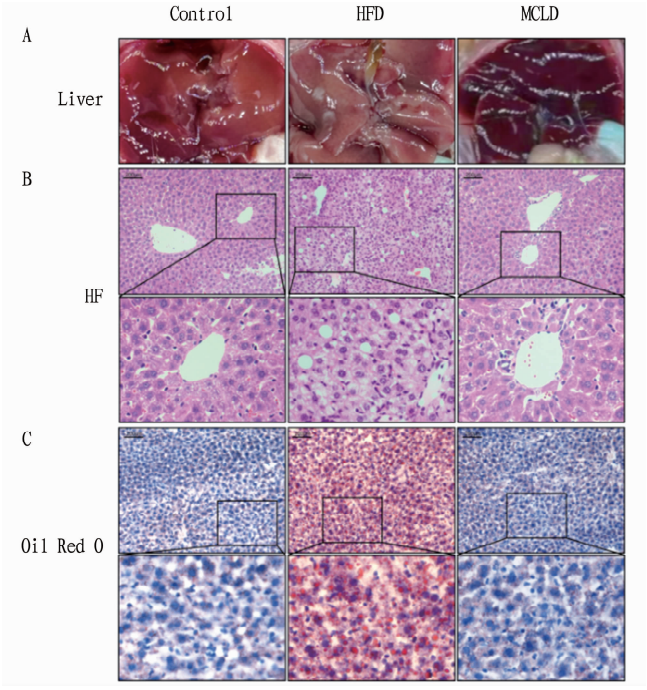
3.1 Hepatic pathological injury and steatosis in mice Histological examination demonstrated that the livers of Control mice were dark red with a glossy surface, while those from the HFD group appeared yellowish and oily (Fig. 1A). H&E staining revealed well-preserved hepatocellular structure and absence of significant steatosis in the Control group, in contrast to the HFD group, which showed disorganized hepatocytes and extensive fatty vacuolation (Fig. 1B). Oil Red O staining further corroborated the presence of conspicuous lipid droplet accumulation in the livers of HFD-fed mice (Fig. 1C). Of note, treatment with MCLD markedly attenuated these histopathological changes.

3.2 Improvement of serum biochemical parameters and hepatic oxidative stress in MASLD mice The results showed that, compared with the Control group, the serum levels of ALT, AST, TG, and TC as well as the hepatic MDA content were significantly elevated in the HFD group, while the hepatic SOD activity and GSH content were markedly decreased. MCLD intervention significantly reversed the above-mentioned indices (Fig. 2). These findings indicate that MCLD can improve liver injury, lipid deposition, and hepatic oxidative stress in MASLD mice.

3.3 MCLD improving HFD-induced hepatic oxidative stress through activation of the Nrf2/HO-1 signaling pathway qRT-PCR results showed that, compared with the Control group, the mRNA expressions of Nfe2l2, Hmox1, and Nqo1 were significantly decreased in the HFD group, while these gene expressions were elevated after MCLD treatment. Western blot results demonstrated that the protein expressions of Nrf2, HO-1, and NQO1 in the HFD group were markedly downregulated relative to the control group, and MCLD intervention increased the above protein expressions (Fig. 3).

4 Discussion

MASLD is now recognized as one of the most common chronic liver diseases globally, characterized by a steadily increasing prevalence and a lack of approved disease-specific medications, thereby representing a major public health concern[13]. The pathological spectrum of MASLD ranges from simple steatosis to metabolic dysfunction-associated steatohepatitis, liver fibrosis, and ultimately hepatocellular carcinoma, yet the underlying mechanisms remain incompletely understood[14-15]. According to the widely accepted "multiple hits" hypothesis, the onset and progression of MASLD are driven by the synergistic interplay of various factors, including lipid overload, oxidative stress, endoplasmic reticulum stress, and mitochondrial dysfunction, with oxidative stress serving as a critical pathogenic hub that links disordered lipid metabolism to hepatocellular damage[16]. Therefore, bolstering antioxidative defenses has emerged as a key therapeutic strategy for MASLD. In the present work, we utilized a HFD-induced mouse model of MASLD to comprehensively assess the therapeutic efficacy of MCLD, verified its beneficial effects against the disease, and provided preliminary evidence for its mechanism involving activation of the Nrf2 signaling pathway.

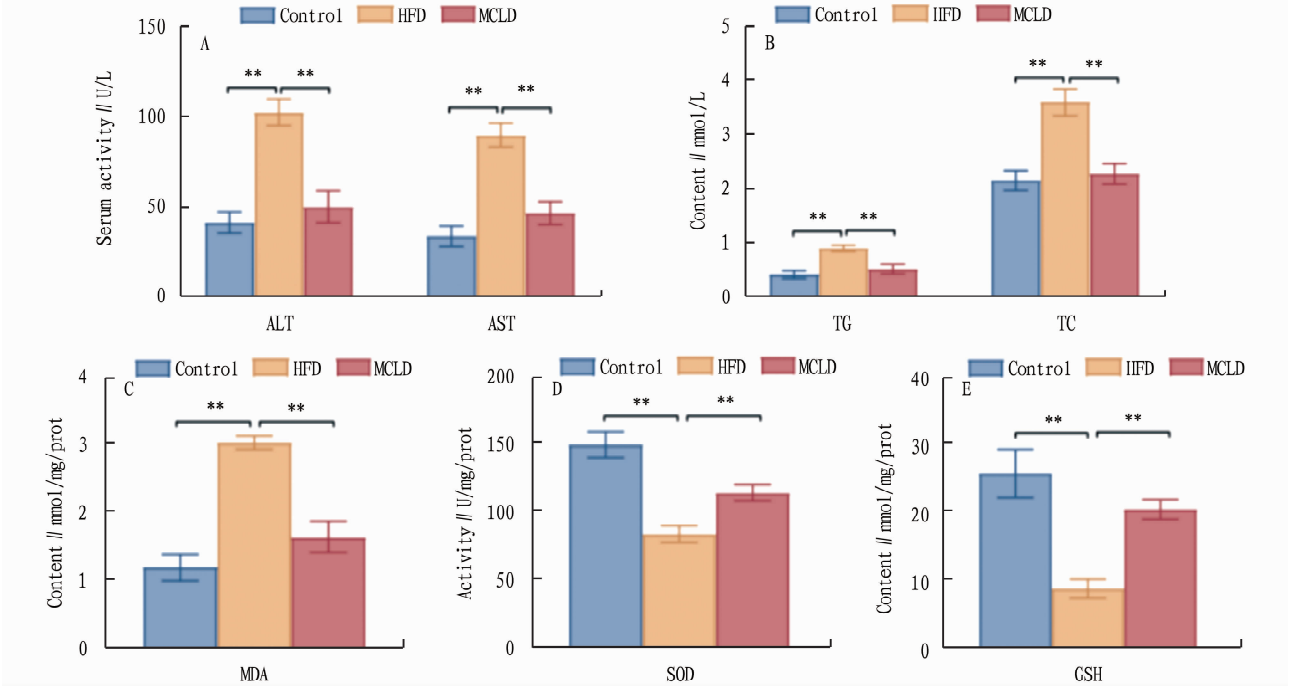


NOTE A. Gross appearance of mouse livers; B. H&E staining of liver tissues; C. Oil Red O staining of liver tissues. Data are expressed as mean ± SD, $n = 6$, scale bar = 200 μm.

Fig. 1 MCLD improves HFD-induced hepatic pathological injury and steatosis in mice

In terms of histopathology, MCLD treatment substantially improved the gross appearance of mouse livers, markedly attenuated hepatocellular steatosis, and reduced lipid droplet accumulation, accompanied by concurrent decreases in serum transaminase and lipid levels. These findings are in line with previous clinical studies on Chaishao Liujunzi Decoction-based formulas for the treatment of metabolic dysfunction-associated fatty liver disease with the liver-stagnation and spleen-deficiency pattern, further corroborating the therapeutic efficacy of this prescription in ameliorating hepatic fat deposition and improving liver function. Of particular note, MCLD also lowered hepatic MDA content while restoring SOD activity and GSH levels, indicating that its hepatoprotective action is mediated, at least in part, by strengthening antioxidative defenses.

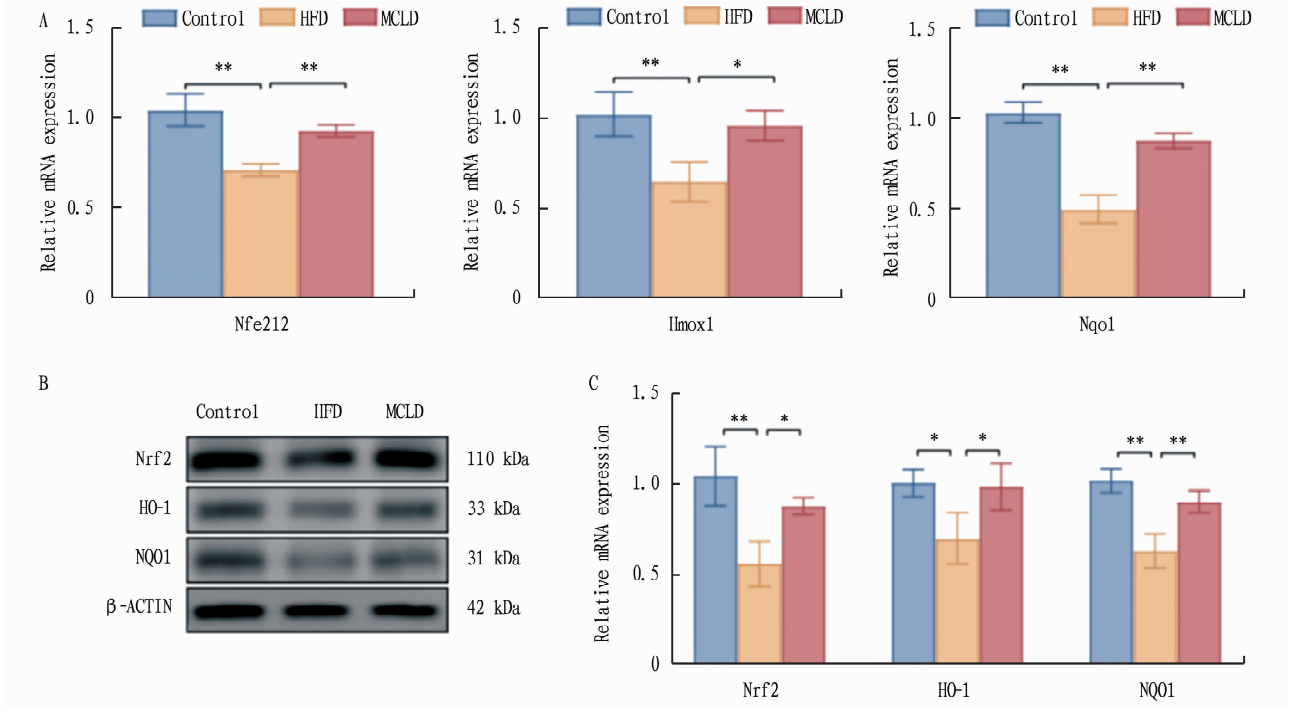
At the molecular level, our study revealed a marked suppression of Nrf2 and its downstream effectors HO-1 and NQO1 in the livers of MASLD mice, a finding that aligns with previous reports demonstrating diminished Nrf2 pathway activity in the MASLD state[17-18]. Following MCLD treatment, both the mRNA and protein expression of these molecules were significantly elevated, indicating that this formula effectively activates the Nrf2 pathway. As the master regulator of cellular antioxidant responses, Nrf2, once activated, orchestrates the transcription of a battery of downstream target genes. In particular, HO-1 catalyzes the degradation of heme into biliverdin and bilirubin, which act as direct free-radical



NOTE A. Serum ALT and AST activities; B. Serum TG and TC levels; C. Hepatic MDA content; D. Hepatic SOD activity; E. Hepatic GSH content. Data are expressed as mean ± SD. $n = 6$, $^{*}P < 0.05$, $^{**}P < 0.01$.

Fig. 2 MCLD improves serum biochemical parameters and hepatic oxidative stress in MASLD mice

scavengers, whereas NQO1 reduces toxic quinones to the less reactive hydroquinones; together, these two enzymes serve as a crucial safeguard against oxidative injury[19]. Our data suggest that MCLD potentiates hepatic ROS clearance and detoxification capacity via this signaling axis, thereby counteracting oxidative stress-driven hepatocellular damage. Corroborating our observations,



NOTE A. mRNA expression of Nfe2l2, Hmox1, and Nqo1 in liver tissues; B-C. Protein expression of Nrf2, HO-1, and NQO1 in liver tissues. Data are expressed as mean ± SD. $n=3$, $^{*}P<0.05$, $^{**}P<0.01$.

Fig. 3 MCLD improving HFD-induced hepatic oxidative stress through activation of the Nrf2/HO-1 signaling pathway

an increasing number of natural products and traditional Chinese medicine formulas have recently been reported to improve MASLD through Nrf2 pathway activation[20-22]. In contrast to these single-agent entities, MCLD is a multi-herb formulation whose characteristic synergistic actions on the Nrf2 pathway may endow it with broader regulatory benefits.

This study demonstrates that MCLD has notable therapeutic efficacy and promising application potential for the treatment of MASLD. Mechanistically, MCLD activates the hepatic Nrf2/HO-1/NQO1 antioxidant signaling axis, upregulates the expression of downstream antioxidant enzymes and phase II detoxifying enzymes, and potentiates hepatic antioxidant defenses, consequently attenuating lipid peroxidative injury, improving liver function, and correcting lipid metabolism disturbances (Fig. 4). While encouraging results were achieved in the *in vivo* setting, the efficacy of MCLD in *in vitro* systems and clinical trials remains to be further investigated.

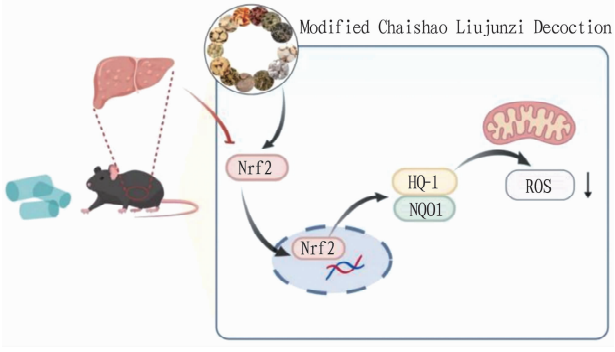


Fig. 4 MCLD activating the Nrf2/HO-1/NQO1 signaling pathway to inhibit hepatic oxidative response

5 Conclusions

In conclusion, these findings demonstrate that MCLD ameliorates HFD-induced MASLD via activation of the Nrf2/HO-1/NQO1 signaling axis, which enhances hepatic antioxidative capacity and attenuates lipid peroxidative injury (Fig. 4). Our study not only provides *in vivo* experimental support for the therapeutic use of MCLD against MASLD, but also proposes a new strategy for MASLD intervention through Nrf2 pathway targeting. Future investigations may employ Nrf2-knockout mice or specific pathway inhibitors to further verify that this signaling cascade constitutes the critical mediator of the hepatoprotective action of MCLD.

References

[1] TILG H, PETTA S, STEFAN N, *et al*. Metabolic dysfunction-associated steatotic liver disease in adults: A review[J]. JAMA, 2026, 335(2): 163-174.

[2] LI W, ALAZAWI W, LOOMBA R. Current and emerging therapeutic landscape for metabolic dysfunction-associated steatohepatitis[J]. The Lancet Gastroenterology & Hepatology, 2026, 11(2): 150-162.

[3] ZHAO K, ZHANG H, DING W, *et al*. Adipokines regulate the development and progression of MASLD through organellar oxidative stress[J]. Hepatology Communications, 2025, 9(2): e0639.

[4] DALLIO M, SANGINETO M, ROMEO M, *et al*. Immunity as cornerstone of non-alcoholic fatty liver disease: the contribution of oxidative stress in the disease progression[J]. International Journal of Molecular Sciences, 2021, 22(1): 436.

[5] CLARE K, DILLON JF, BRENNAN PN. Reactive oxygen species and oxidative stress in the pathogenesis of MAFLD[J]. Journal of Clinical and Translational Hepatology, 2022, 10(5): 939 – 946.
[6] ZHANG DD. Thirty years of NRF2: Advances and therapeutic challenges [J]. Nature Reviews Drug Discovery, 2025, 24(6): 421 – 444.
[7] MANAVI MA, MOHAMMAD JAFARI R, SHAFAROODI H, *et al.* The Keap1/Nrf2/ARE/HO-1 axis in epilepsy: Crosstalk between oxidative stress and neuroinflammation[J]. International Immunopharmacology, 2025, 153: 114304.
[8] SHRESTHA J, LIMBU KR, CHHETRI RB, *et al.* Antioxidant genes in cancer and metabolic diseases: Focusing on Nrf2, sestrin, and heme oxygenase 1[J]. International Journal of Biological Sciences, 2024, 20 (12): 4888 – 4907.
[9] ROSS D, SIEGEL D. The diverse functionality of NQO1 and its roles in redox control[J]. Redox Biology, 2021, 41: 101950.
[10] YANG K, YU X, GUO Z, *et al.* PIM1 alleviated liver oxidative stress and NAFLD by regulating the NRF2/HO-1/NQO1 pathway[J]. Life Sciences, 2024, 349: 122714.
[11] GU X, LUO Y, ZHANG J, *et al.* The therapeutic role of natural compounds mediated through Nrf2 in metabolic dysfunction-associated steatotic liver disease[J]. Biochemical Pharmacology, 2026, 250(Pt 1): 117989.
[12] WANG C, LIU K, JI J, *et al.* Liu-Jun-Zi decoction alleviates metabolic dysfunction-associated steatohepatitis by modulating myogenic irisin mediated skeletal muscle-liver crosstalk[J]. Phytomedicine, 2025, 148: 157218.
[13] LAU HC, ZHANG X, YU J. Gut microbiome in metabolic dysfunction-associated steatotic liver disease and associated hepatocellular carcinoma [J]. Nature Reviews Gastroenterology & Hepatology, 2025, 22(9): 619 – 638.
[14] MIAO L, TARGHER G, BYRNE CD, *et al.* Current status and future trends of the global burden of MASLD[J]. Trends in Endocrinology & Metabolism, 2024, 35(8): 697 – 707.
[15] KAMZOLAS I, KOUTSANDREAS T, BARKER CG, *et al.* A data-driven framework reconstructs the molecular continuum of human MASLD progression[J]. Nature Metabolism, 2026, 8(7):1545 – 1562.
[16] LOOMBA R, FRIEDMAN SL, SHULMAN GI. Mechanisms and disease consequences of nonalcoholic fatty liver disease[J]. Cell, 2021, 184 (10): 2537 – 2564.
[17] LIU P, ANANDHAN A, CHEN J, *et al.* Decreased autophagosome biogenesis, reduced NRF2, and enhanced ferroptotic cell death are underlying molecular mechanisms of non-alcoholic fatty liver disease[J]. Redox Biology, 2023, 59: 102570.
[18] YIN X, LIU Z, LI C, *et al.* Hinokitiol ameliorates MASH in mice by therapeutic targeting of hepatic Nrf2 and inhibiting hepatocyte ferroptosis [J]. Phytomedicine, 2025, 139: 156472.
[19] CHEN WT, MCKEE NW, KUHNELL D, *et al.* NRF2: Master regulator of cellular homeostasis and therapeutic vulnerability in cancer[J]. Redox Biology, 2026, 90: 104050.
[20] LI Y, YE M, HE Q, *et al.* Novel dual AMPK/NRF2 activation by leucocyanidin from Hawthorn (*Crataegus*) for mitochondria repair-targeted therapy of hepatic steatosis[J]. Phytomedicine, 2026, 150: 157614.
[21] YU CHJ, RUPASINGHE HPV. Elucidating the mechanistic interplay of AMPK and Nrf2 in MASLD: A focus on dietary phytochemical modulation of lipid and redox homeostasis[J]. Biochemical and Biophysical Research Communications, 2025, 777: 152300.
[22] LIU L, BAI Y, LIU X, *et al.* Panax notoginseng saponins alleviates metabolic dysfunction-associated steatotic liver disease in mice by influencing Nrf2/MT2[J]. Frontiers in Pharmacology, 2026, 17:1874424.

(From page 63)

relative to the model group. These findings suggest that Jianpi Huashi Granules may exert its therapeutic effects by modulating VIP and VIP R1 expression, thereby regulating aquaporin activity, reducing membrane permeability, and attenuating gastrointestinal motility, which in turn alleviates D-IBS-associated abdominal pain and intestinal dysfunction. On this basis, we hypothesize that the involvement of spleen deficiency and liver depression syndrome in D-IBS pathogenesis may be attributable to brain-gut axis dysregulation, with the underlying material basis reflected in altered levels of brain-gut peptides including VIP and VIP R1.

References

[1] XIE BY, SHAO Z, LI SJ. Effect of Nesfatin-1 on colonic motility and CRF signaling pathway in IBS-D model rats[J]. Modern Practical Medicine, 2024, 36(4): 438 – 442. (in Chinese).
[2] CHAO GQ. The change of intestinal mucous membrane aquaporins of diarrhea-predominant irritable bowel syndrome and its molecular mechanism study[D]. Hangzhou: Zhejiang University, 2018. (in Chinese).
[3] MEARIN F, LACY BE, CHANG L, *et al.* Bowel disorders[J]. Gastroenterology, 2016, 150:1393 – 1407.
[4] WANG Y, BAO XL, LANG YX, *et al.* Effects of interstitial cells of Cajal changes on gastrointestinal motility and levels of VIP and CGRP in experimental diarrhea-predominant irritable bowel syndrome model rats[J]. Chinese Journal of Gerontology, 2021, 41(6): 1293 – 1296. (in Chinese).
[5] AGIRMAN G, YU KB, HSIAO EY. Signaling inflammation across the gut-brain axis[J]. Science, 2021, 374(6571): 1087 – 1092.
[6] XU HZ, XIE JQ, SHI B, *et al.* Expression of inflammatory cytokine in colon mucosa of D-IBS rats and effects of "Wenzhong Jianpi Decoction" on them[J]. Shanghai Journal of Traditional Chinese Medicine, 2007 (6): 69 – 72. (in Chinese).
[7] WANG YH, LIU YL, ZHAO SW, *et al.* Correlation between D-IBS with spleen deficiency and liver stagnation symptoms and 5-HT,CRH[J]. Chinese Journal of Experimental Traditional Medical Formulae, 2017, 23 (18): 124 – 129. (in Chinese).
[8] EL-SALHY M. Recent developments in the pathophysiology of irritable bowel syndrome[J]. World Journal of Gastroenterology, 2015, 21(25): 7621 – 7636.
[9] ZHANG SS, WEI W, YANG JQ. Consensus opinion of traditional Chinese medicine diagnosis and treatment of irritable bowel syndrome (2017)[J]. Journal of Traditional Chinese Medicine, 2017, 58(18): 1614 – 1620. (in Chinese).
[10] SONG YL. Effects of Jianpi Anchang Pill on VIP and SP of brain-gut peptide in D-IBS rats model[D]. Jinan: Shandong University of Traditional Chinese Medicine, 2017. (in Chinese).
[11] ZHANG Y, LI P. The research progress of vasoactive intestinal peptide [J]. Medical Recapitulate, 2009, 15(21): 3235 – 3238. (in Chinese).
[12] LI RF, WANG DS, WANG YJ, *et al.* Pinaverium bromide for diarrhea-predominant irritable bowel syndrome rat model with colonic tissue vasoactive intestinal peptide and its expression of receptor 1[J]. Chinese Journal of Integrated Traditional and Western Medicine on Digestion, 2010, 18(2): 89 – 92. (in Chinese).
[13] LIU ZW, YU JJ, MA XR, *et al.* Changes of colonic tight junction proteins, AQP3 and AQP4 in IBS-D model rats with liver depression and spleen deficiency syndrome[J]. Chinese Journal of Gerontology, 2023, 43(24): 6044 – 6047. (in Chinese).